SUPPLEMENTARY FIGURES AND LEGENDS

Figure S1 (related to Figure 1)

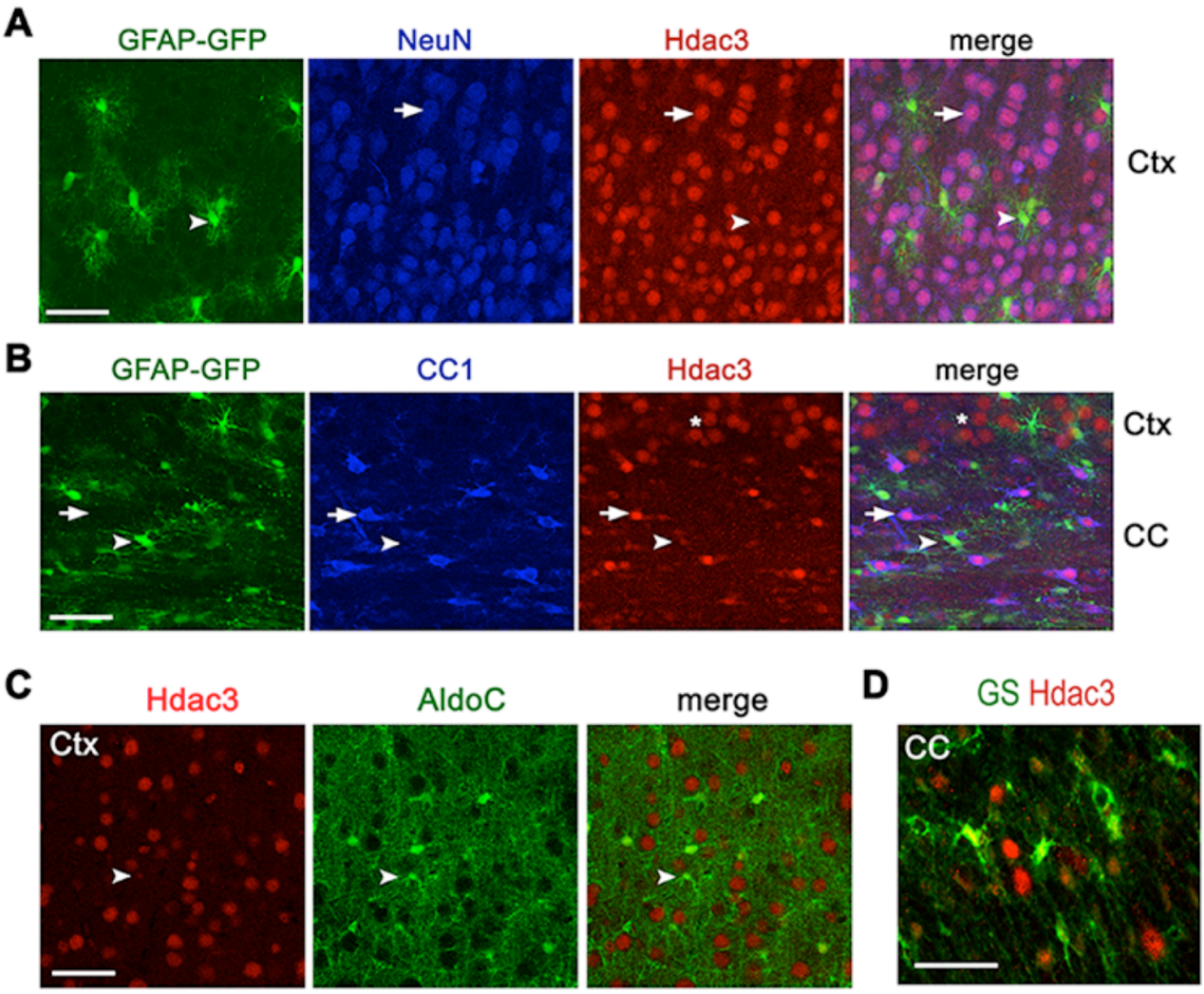

Figure S1 (related to Figure 1). Hdac3 is expressed at a low level in astrocytes in the developing brain

(A-D) Sections of the brain from the mice carrying the GFAP-GFP transgene at P7 was immunostained with antibodies to NeuN, CC1, AldoC, GS and Hdac3 as indicated.

Arrowheads indicate GFAP-GFP^{+} or AldoC^{+} astrocytes in panels A-C.

Arrows in panel A and B indicate neurons and CC1+ oligodendrocytes, respectively.

* in B indicates cortical neurons above the corpus callosum.

Ctx: cortex (panels A and C); CC: corpus callosum (panels B and D). Scale bars, 40 μm.

Figure S2 (related to Figure 2)

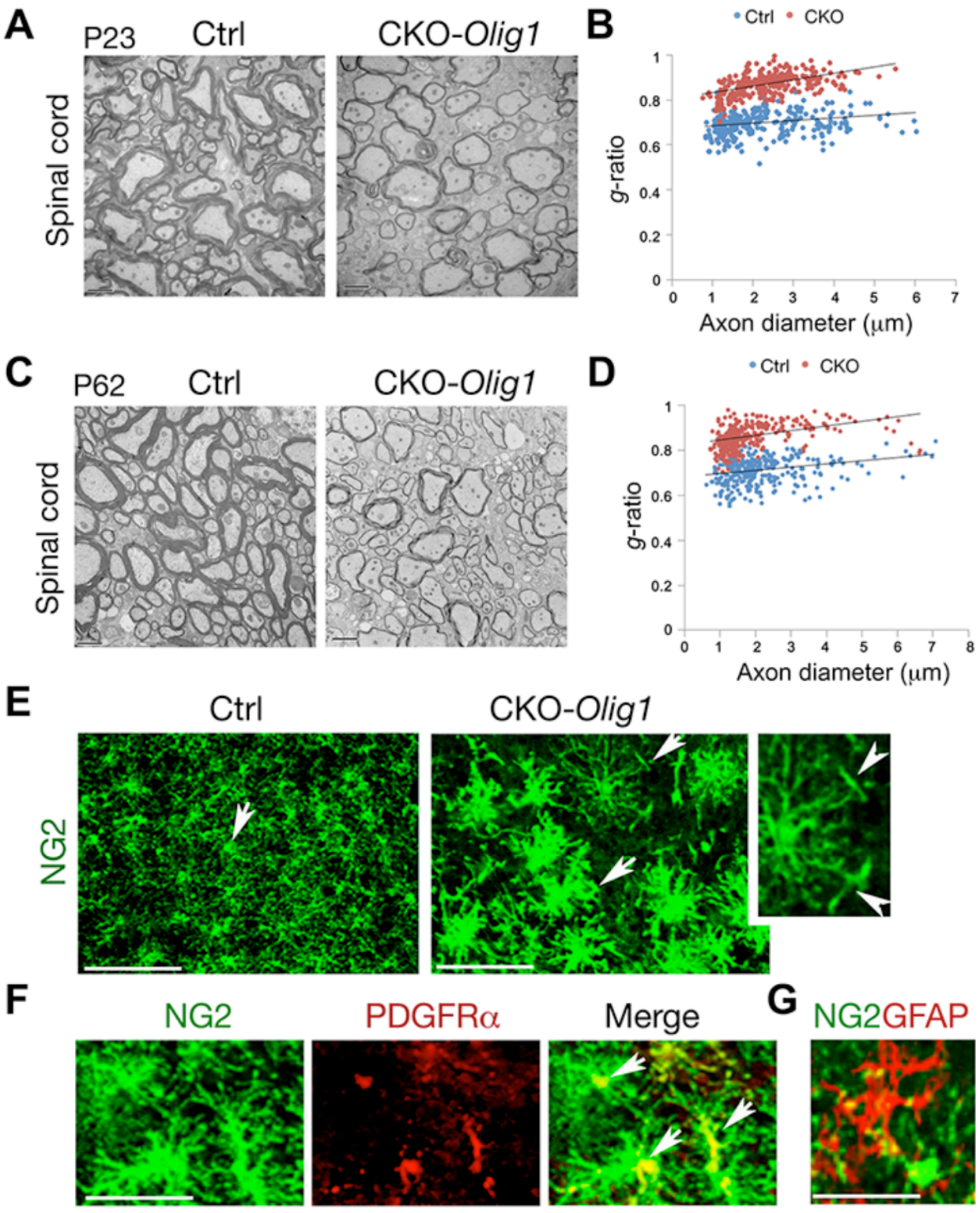

Figure S2 (related to Figure 2). Myelin assembly defects and abnormal morphology of NG2$^+$ cells in the CNS of Hdac3 mutant mice

(A,C) Electron micrographs of ventral spinal white matter from control and CKO-*Olig1* mice at P23 (A) and P62 (C) as indicated.

(B,D) Quantification of g-ratios as a function of axon diameter at P23 and P62 as indicated. There

was a significant difference between control and mutant (n = 3 animals/genotype; $^{**}p < 0.01$, Student's *t*-test).

(E) The cortex of control and CKO-*Olig1* mice was immunostained with anti-NG2 at P14. Arrows indicate immunolabeled cells. Arrowheads in inset indicate potential perpendicular $NG2^+$ processes around axons.

(F) The cortex of control and CKO-*Olig1* mice was immunostained with anti-NG2 and anti-PDGFRα at P14. Arrows indicate co-immunolabeled cells.

(G) The cortex of CKO-*Olig1* mice was immunostained with anti-NG2 and anti-GFAP at P14. A representative image showing that NG2 and GFAP immunolabeled cells were not overlapped. Similarly, we did not observe NG2/GFAP co-labeling in the cortex of CKO-*Olig1* mice in adulthood at P60.

Scale bars in A, C; 2 μm; E-G, 50 μm.

Figure S3 (related to Figure 3)

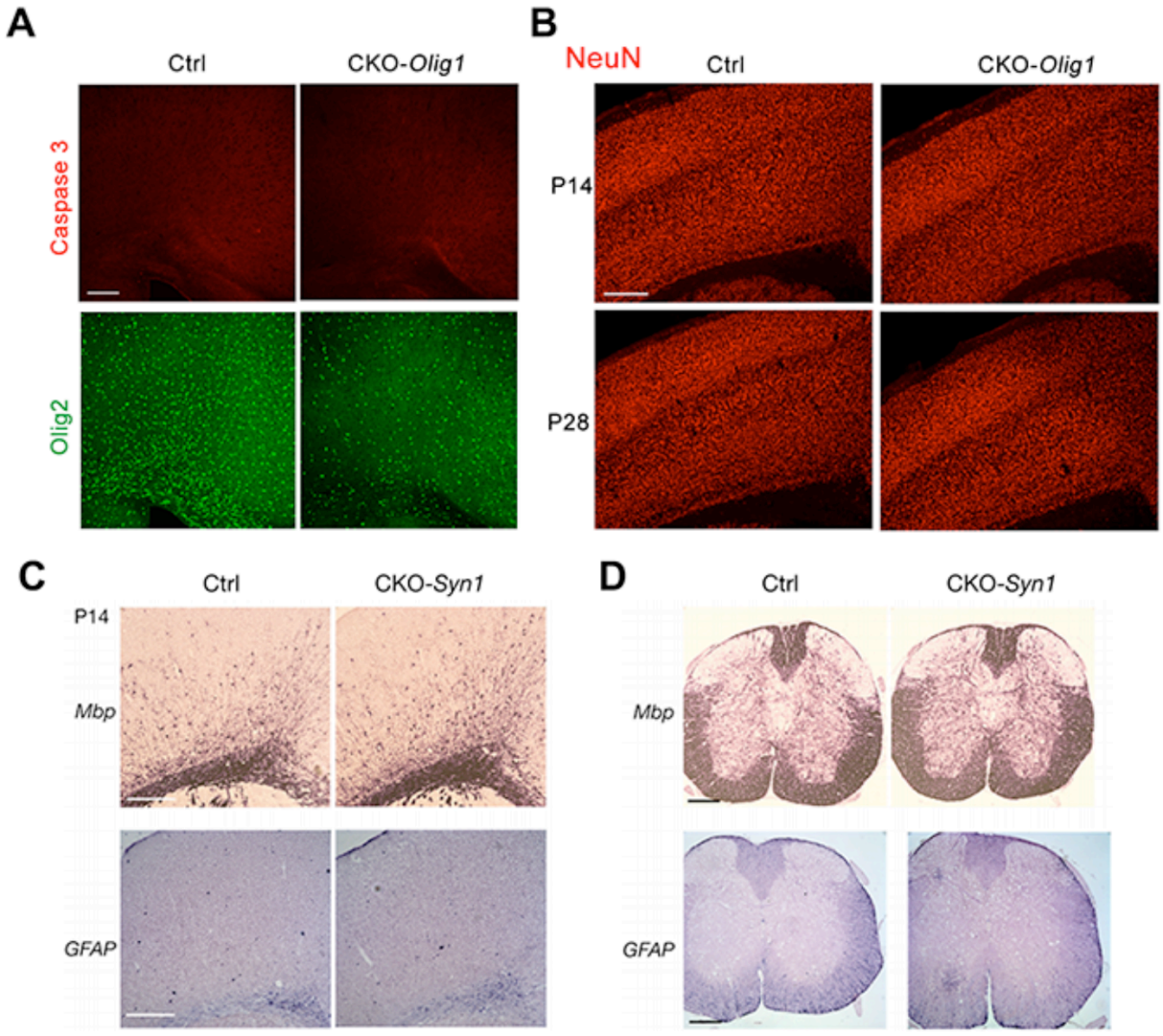

Figure S3 (related to Figure 3). Effects of *Hdac3* ablation on cell survival and neuronal development

(A) Cortical sections of the brains from control (Ctrl) and *Hdac3* mutant mice (CKO-*Olig1*) at P28 were immunostained with antibodies to an active form of Caspase 3 and Olig2.

(B) Cortical sections of the brains from control and CKO-*Olig1* mutant mice at P14 and P28 were immunostained with antibodies to NeuN. Representative images were shown.

(C,D) Cortical sections of brains (C) and transverse spinal cords (D) from control and Hdac3 CKO-*Syn1-Cre* mice at P14 were subject to in situ hybridization with probes to *Mbp* and *GFAP* as indicated. Representative images were shown.

Scale bars in A, B; 100 μm; C, D, 200 μm.

Figure S4 (related to Figure 3)

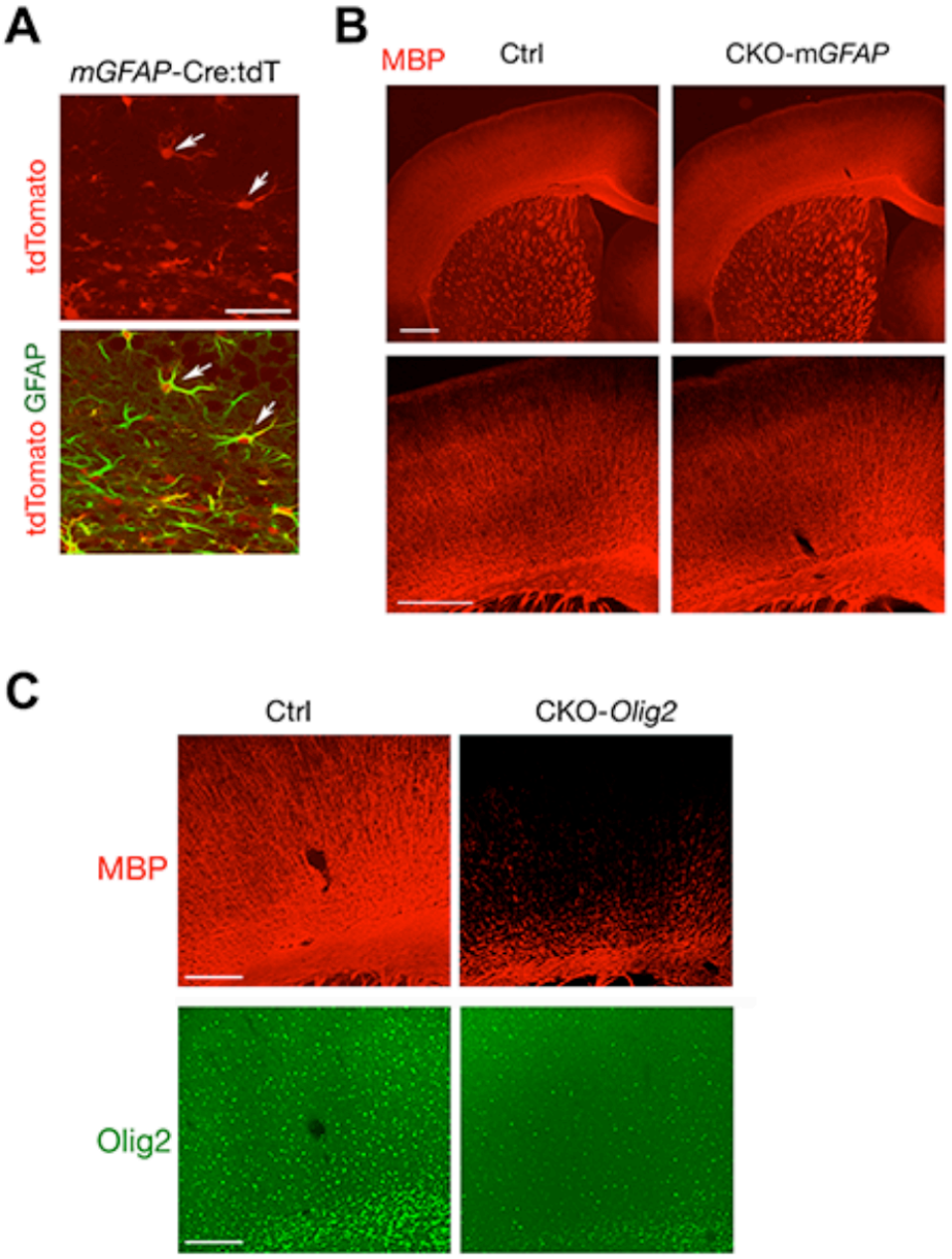

Figure S4 (related to Figure 3). Effects of *Hdac3* ablation in astroglial and Olig2-expressing cells

(A) The progeny of mGFAP-Cre-expressing cells label GFAP$^+$ astrocytes. A cortical section of the brain from *mGFAP-Cre*$^{+/-}$:CAG-tdTomato reporter mice at P21 was immunostained with the antibody to GFAP and visualized with tdTomato signals. Arrows indicate GFAP$^+$/tdTomato$^+$ astrocytes.

(B) Cortical sections of brains from control and CKO-m*GFAP* (*mGFAP-Cre*$^{+/-}$:*Hdac3*$^{lox/lox}$) mice at P21 were immunostained with antibodies to MBP. Images in the lower panels were shown at a high magnification around the corpus callosum.

(C) Cortical sections of brains from control and CKO-*Olig2* mice at P21 were immunostained with antibodies to MBP and Olig2 as indicated.

Scale bars in A, 50 μm; B, 200 μm; C, 100 μm.

Figure S5 (related to Figure 5)

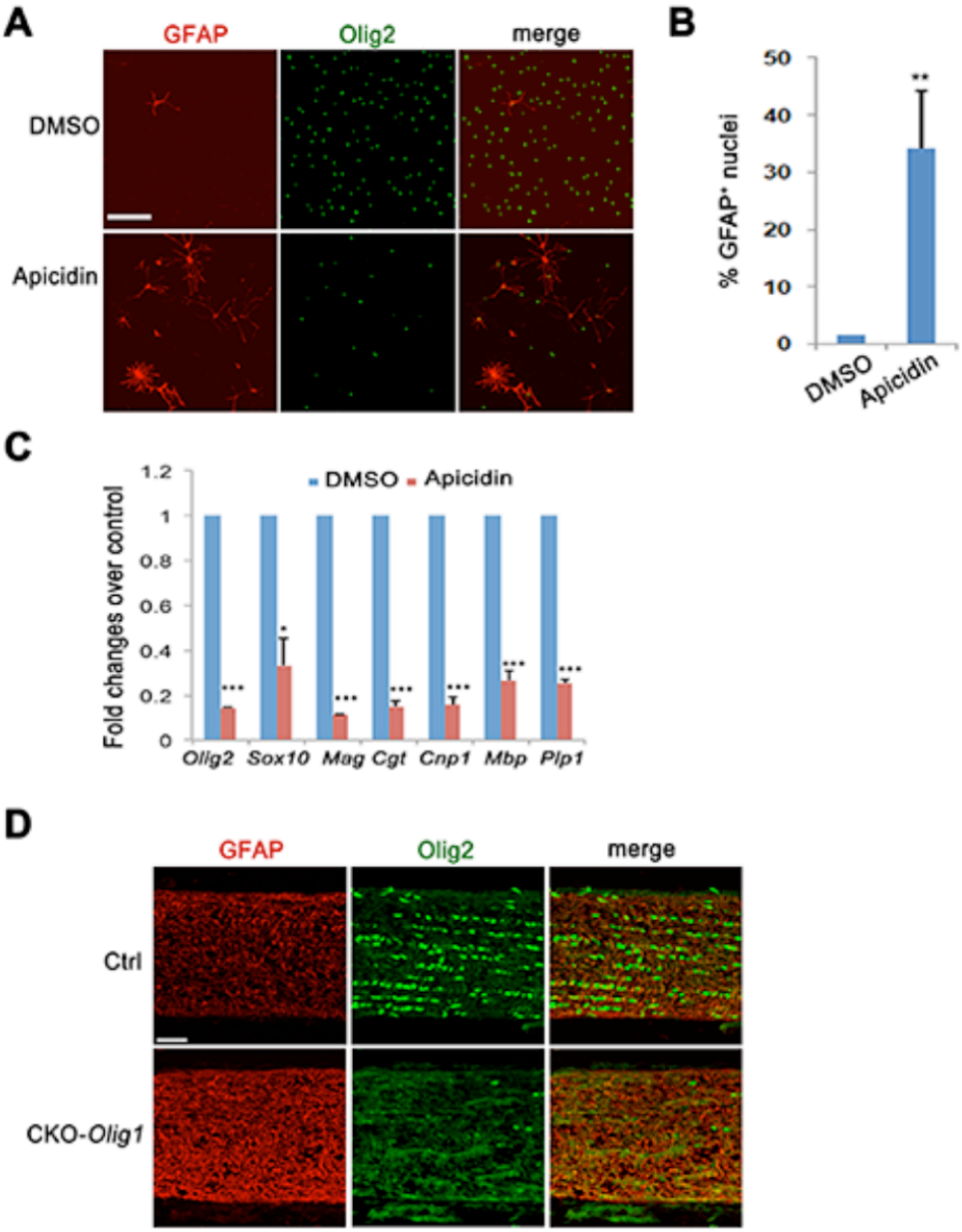

Figure S5 (related to Figure 5). Inhibition of Hdac3 leads to upregulation of astrogliogenesis in vitro and in vivo

(A) Rat primary OPCs were treated with the Hdac3/NCoR inhibitor apicidin (20 nM) for 4 days and immunostained with GFAP and Olig2.

(B) Bar graph depicts the quantification of the percentage of $GFAP^{+}$ astrocytes after treatment with DMSO and apicidin in rat OPCs.

(C) Rat primary OPCs were treated with apicidin (100 nM) for 8 hr and cultured in the T3-containing differentiation medium. Bar graphs depict that relative expression of myelination-associated genes assayed by qRT-PCR in drug- over vehicle-treated cells. Experiments were performed at least three times for each treatment.

(D) The optic nerve of control and CKO-*Olig1* mice at P21 was immunostained with Olig2 and GFAP as indicated. The fluorescent images were acquired with equal offset and gain controls for each channel.

Scale bars in A and D, 50 μm. Data are presented as mean ± S.E.M. in B and C from at least three independent experiments. **p*<0.05, ***p*<0.01, ****p*<0.001; Student's *t*-test.

Figure S6 (related to Figure 6).

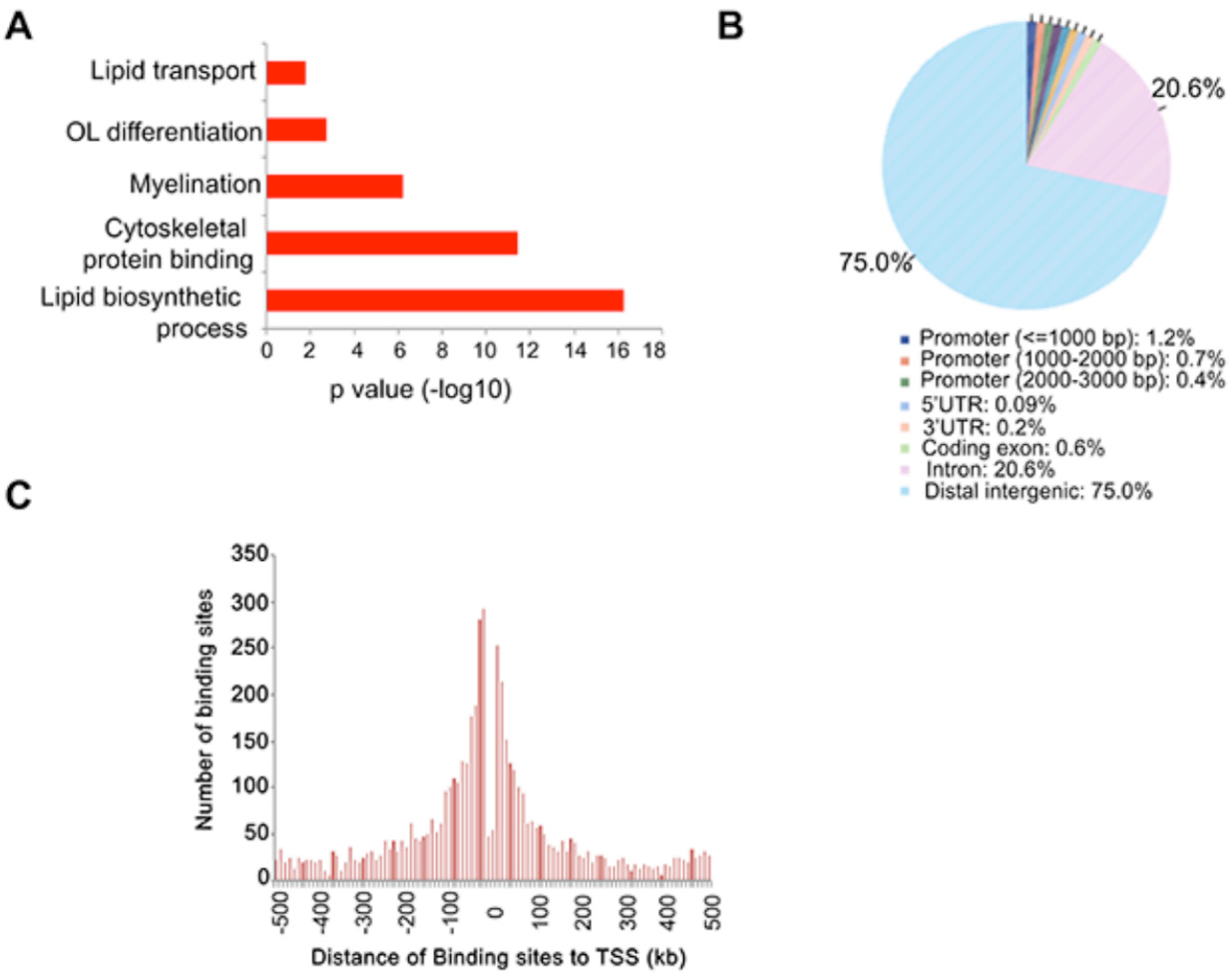

Figure S6 (related to Figure 6). Gene Ontology enrichment analysis of Hdac3-targeted regulatory elements

(A) Gene ontology analysis indicated significant enrichment of the genes associated with myelination, cytoskeleton, and lipid synthesis among the downregulated genes in *Hdac3* mutants (CKO-*Olig1*) as compared to controls.

(B) The pie chart depicts the distribution of Hdac3 binding sites in mOL over different categories of regulatory elements in promoter, UTRs, coding exon, and intron regions.

(C) Histogram showing the distribution pattern of Hdac3-binding regions in mOL mapped to the transcription start site (TSS) of their closest Ensembl annotated genes.

Figure S7 (related to Figure 7)

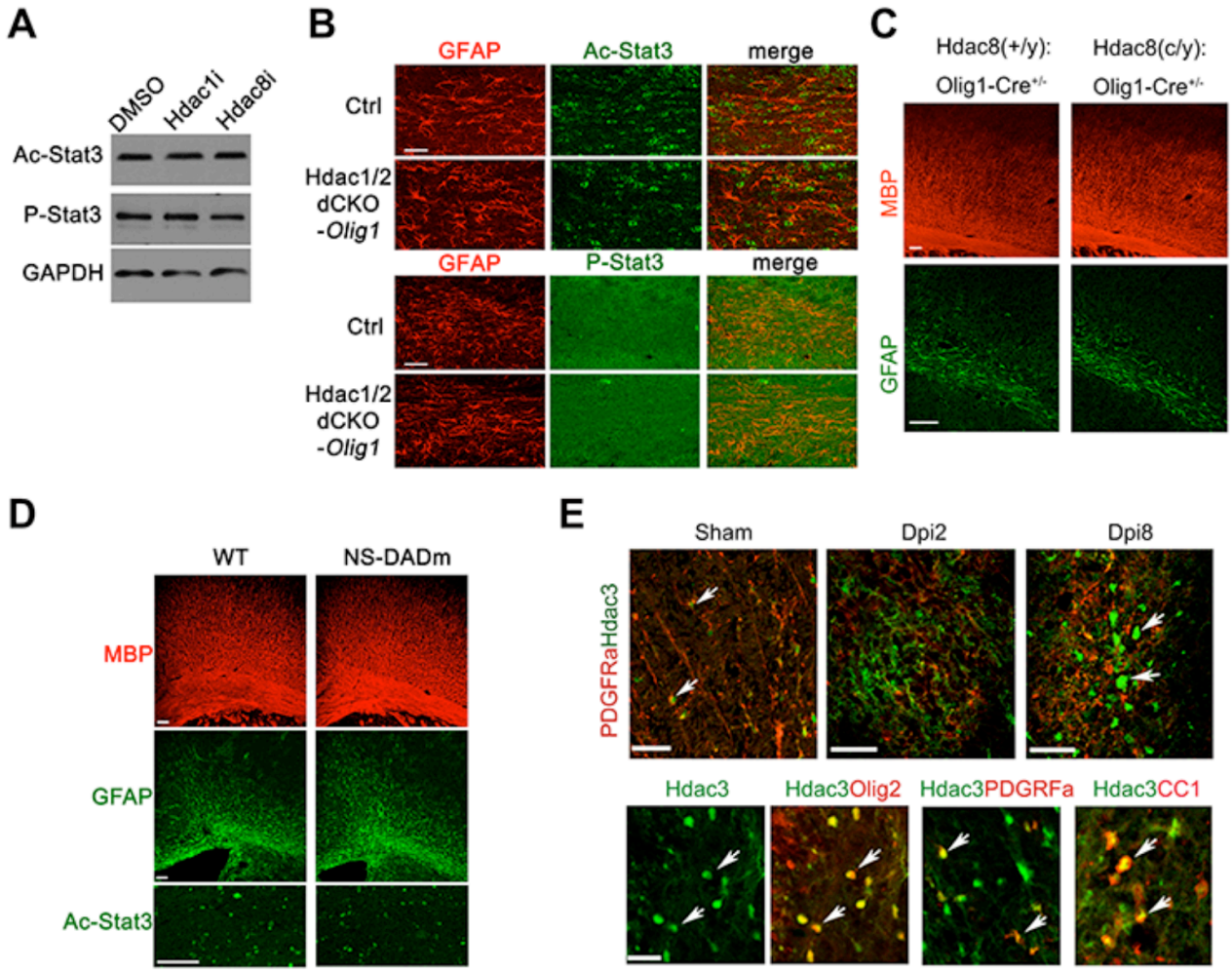

Figure S7, related to Figure 7. Specific role of Hdac3 in regulation of Stat3 post-translational modification and demyelinating injury response

(A) Rat primary OPCs were treated with DMSO, Hdac1i or Hdac8i inhibitor and subject to western blot with antibodies to Ac-Stat3 or P-Stat3 as indicated. GAPDH as loading control.

(B) The corpus callosum of the control and Hdac1/2 dKO-*Olig1* (*Hdac1/2*$^{fl/fl}$*:Olig1-Cre*$^{+/-}$) mice (Ye et al., 2009) at P10 was immunostained with antibodies to Ac-Stat3, P-Stat3 and GFAP as indicated.

(C) Cortical sections of the brains from control (Ctrl; *Hdac8*$^{+/y}$*:Olig1Cre*$^{+/-}$) and *Hdac8* conditional mutant male mice (*Hdac8*$^{fl/y}$*:Olig1Cre*$^{+/-}$) at P28 were immunostained with antibodies to MBP and GFAP. *Hdac 8* is an X-chromosome linked gene. Representative images were shown.

(D) Cortical sections of the brains from wildtype and NS-DADm mutant mice at P15 were immunostained with antibodies to MBP and GFAP. The corpus callosum of wildtype and NS-DADm mutant mice at P15 were immunostained with anti-ac-Stat3 antibody. Representative images were shown.

(E) The ventral spinal cord from vehicle and lysolethicin-treated adult mice was immunostained at different days after lysolecithin injection for Hdac3, PDGFRα, Olig2 and CC1 as indicated days after injury. Upper panel: An increase of Hdac3-expressing cells and signals was detected in

remyelinating lesion (arrows) during the remyelination phase at days post lysolecithin-induced injury (Dpi), Dpi2 and Dpi8. Lower panels: Hdac3 upregulation was detected in $Olig2^+$, $PDGFR\alpha^+$, and $CC1^+$ oligodendrocyte lineage cells in the lesion at Dpi8. Arrows indicate co-labeling cells. Scale bars in B-D, 50 μm; E, upper panels, 50 μm; lower panels; 25 μm.

SUPPLEMENTAL EXPERIMENTAL PROCEDURES

Procedures for tissue processing, antibodies, immunostaining and microscopy: CNS tissues at defined ages were dissected and fixed overnight in 4% (w/v) paraformaldehyde (PFA) and processed for cryosectioning or paraffin embedding and sectioning. The procedure for tissue immunostaining was described previously (Lu et al., 2000). Briefly, for tissue immunostaining, cryosections or pre-deparaffinized tissue sections were incubated overnight in primary antibodies diluted in block solution (PBS with 5% v/v normal goat serum (Sigma-Aldrich) and 0.3% v/v Triton X-100). After washing with PBS five times, sections were then incubated overnight at 4 °C with corresponding fluorophore-conjugated secondary antibodies (Jackson ImmunoResearch) under fluorescent microscopy. For cell immunostaining, cultured cells were fixed with 4% PFA for 10 min and washed five times with PBS, then placed in blocking solution for 30 min. We incubated primary antibodies in blocking solution with proper dilutions and stained cells for 1 h at room temperature. For BrdU staining, cells or tissue sections were denatured with 0.1N HCl for 1 h in 37°C water bath. After denaturation, sections were neutralized with 0.1 M Borax, pH 8.5 (Sigma) for 10 min. Sections were washed with 0.3% Triton X-100/1 × PBS (wash buffer) for 3 times and blocked with 5% normal donkey serum (Sigma-Aldrich) contained wash buffer for 1 h at room temperature. Mouse-anti BrdU (BD Bioscience, 1:500) antibody was used to label BrdU overnight at 4°C. DAPI was included in the final washes before the samples were mounted in Fluoromount G (SouthernBiotech) for microscopy. Primary antibodies used in this study were as follows: Olig2 (Millipore AB9610), GFAP (Sigma, G3893), Ki67 (Thermo Sci, Clone: SP6), BrdU (BD Bioscience 347580), NeuN (Millipore, MAB377), PDGFRα (BD Pharmingen 558774), MBP (Santa Cruz sc-13914), CC1 (Calbiochem OP80), Hdac3 (Abcam ab7030 for ChIP-seq), NG2 (Millipore MAB5384), Glutamine synthetase (Millipore MAB302), S100β (Sigma S2532), GFP (Abcam Ab455), Stat3 (Cell Signaling 9139), P-Stat3 (Cell signaling 9145), Ac-Stat3 (Cell signaling 2523), Sox10 (Santa Cruz sc-17342), NFIA (gift from Dr. Ben Deneen, Baylor College of Medicine) and Caspase 3 (Cell Signaling 9661), Aldh1l1 (Abcam Ab56777) and AldoC (Santa Cruz sc-12065).

For microscopy and image acquisition, images of stained samples were collected on an inverted laser scanning confocal microscope (Nikon C2 confocal System) microscope equipped with high-efficiency fluorochrome specific filter sets for DAPI, Cy2, Cy3 and Cy5. For

quantification of the immuno-labeled cells, areas to be counted were traced with a 40× objective lens and at least 10 random but non-overlap regions per section sample frames (40 μm × 40 μm) were selected by the imaging analysis software. At least five sections at different hindbrain levels per animal were selected for quantification. Experiments were performed at least three times for each genotype. Images were quantified in a double-blinded manner.

RNA *in situ* hybridization of brain sections was performed using digoxigenin-labeled riboprobes as described previously (Lu et al., 2002). The probes used were: murine *Mbp, Plp1* and *PDGFRα.* Detailed in situ protocols are available upon request.

Real-time RT-PCR Analysis: RNAs were isolated with the Trizol (Invitrogen Inc.) from cells or snap-frozen tissues. Reverse transcription was performed with cDNA Reverse Transcription Kit (Bio-Rad) with iQ™ SYBR® Green Supermix (#170-8880). We analyzed each gene with two different primer sets. qRT-PCR was carried out using the ABI Prism 7900 Sequence Detector System (Perkin-Elmer Applied Biosystems) using *Gapdh* as an internal control. Each analysis was performed in triplicates, and the results were normalized to *Gapdh* for each sample. The primer sequences for qRT-PCR of rat genes are *Hdac3-f, tgtctcaatgtgcccttacg; Hdac3-r, cctaatc gatcacagcccag; Gapdh-f, tccagtatg actctacccacg; Gapdh-r, cacgacatactcagcaccag; GFAP-f, gactttctccaacctccagatc; GFAP-r, ctcctgcttcgactccttaatg; Id2-f, atggaaatcctgcagcacgtcatc; Id2-r, acgtttggttct gtccaggtctct; Hes5-f, accagccca actccaaac; Hes5-r, agtaaccctcgctgtagtcc; Pdgfra-f, tgtggactctgac aacgcgtacat; Pdgfra-r, atctctgttcatccag gccacctt; Id4-f, actgtgcctgcagtgcgatatgaa; rat Id4-r, tgcaggatctccactttgctgact; Cgt-f, agataaagatgggcggccgttact; Cgt-r, tatttgaggtgctcctgccggtta; Mag-f, acagcgtcctggacatcatcaaca; Mag-r, atgcagctgacctctactccgtt; Sox10-f, gctatccaggctcactacaag; Sox10-r, actgcagctctgtctttgg; Olig2-f, gcgcgatgctaagctctttgttca; Olig2-r, tgtatgggccacgacacagaaaga. For mouse genes, mCNTF-f, tgacctccgtgtcatttcttc; mCNTF-r, ggagacagaggcaagagttaag; CT1-f, cttcccaccagttcctttgtag, mCT1-r, ctgcctttctctctccattgac*.

Western blot analysis and co-immunoprecipitation: Isolated cells or tissues were lysed in modified RIPA buffer (50 mM Na-Tris, pH 7.4, 150 mM NaCl, 1% (v/v) NP-40, 0.25% sodium deoxycholate, 1 mM dithiothreitol, 10 mM NaF, 1 mM active sodium vanadate, 1 mM PMSF and 1 x a cocktail of cOmplete protease inhibitors (Roche Applied Science) and centrifuged at 13,000 rpm for 15 min at 4 °C. After protein concentration was determined (Bio-Rad), the lysates were separated by 4–12% SDS-PAGE. We performed western blotting using standard protocols.

Co-immunoprecipitation and immunoblotting were performed as described previously (Weng et al., 2012). Briefly, a total of 300 μg of protein lysates from transfected cells were pre-cleaned using protein A-sepharose and then immunoprecipitated with 2 μg antibody for co-immunoprecipitation.

Procedures for primary OL cell culture and transfection: Primary rat OPCs were isolated from cortices of pups at P2 using a differential detachment procedure as previously described (Chen et al., 2007). Briefly, mixed glial cells were cultured in 15% FBS medium for five to seven days, then switched to B104 conditional medium for 2 days prior to isolating OPCs by mechanical dissociation in an orbital shaker. Isolated rat OPCs were collected or grown in the OPC growth medium (Sato medium supplemented mitogens 10 ng/ml PDGF-AA and 20 ng/ml bFGF), and differentiated in oligodendrocyte differentiation medium (Sato medium supplemented with 15 nM thyroid hormone T3 (triiodothyronine) and 10 ng/ml ciliary neurotrophic factor) for 24 hr and 72 hr to become iOL and mOL as the initiation and maturing phases of oligodendrocytes, respectively, as previously described (Yu et al., 2013). Mouse OPCs were isolated from P7-8 cortices of control and mutants by immunopanning with antibodies Ran-2, GalC, and PDGFRα sequentially as previously described (Chan et al., 2004). Astrocytes were isolated and cultured as previously described (Chen et al., 2007; McCarthy and de Vellis, 1980): Briefly, confluent monolayer mixed glial culture was shaken vigorously to remove loosely attached microglia and OPCs. Cells were then passaged after dissociation with trypsin/EDTA. Rat OPCs or astrocytes were transfected with expression vectors by using Amaxa Nucleofector (Lonza) according to the manufacturer's protocol. Expression vectors for Hdac3 and Hdac3-HEBI were kindly provided by Dr. Zheng Sun (Univ. Pennsylvania). Hdac inhibitors: HDAC1 inhibitor (CI994, Selleckchem Inc.), HDAC8 inhibitor (PCI30451, Selleckchem Inc.), HDAC3 inhibitor (RGFP966, Selleckchem Inc) or Apicidin, an inhibitor of HDAC3 and N-CoR (Santa Cruz Biotechnology).

Procedures for Chromatin immunoprecipitation (ChIP)-sequencing: ChIP-seq assays were performed as previously described with minor modifications (Yu et al., 2013). Briefly, OPCs and oligodendrocytes at different stages (~20 million cells) were fixed for 10 min at room temperature with 1% formaldehyde-containing medium. Nuclei were pelleted and sonicated in sonication buffer (10 mM Tris-HCl, pH 8.0, 1 mM EDTA, 0.5 mM EGTA and protease inhibitor cocktail). Nuclear suspensions were sonicated with a Covaris S220 sonicator. Sonicated chromatin (~300 μg) was used for immunoprecipitation by incubated with appropriate antibodies (4 μg) overnight at 4 °C.

10% of chromatin used for each ChIP reaction was kept as input DNA. Pre-rinsed protein A/G plus agarose beads (50 μl) was added to each ChIP reaction and incubated for 1 hr at 4 °C. The beads were then incubated in 200 μl elution buffer at 65 °C for 20 min to elute immunoprecipitated materials. The ChIP-seq libraries were prepared using 5500 SOLiD Fragment Library Core Kit (PN 4464412) as recommended by the manufacturer. They were then run on the 5500xl SOLiD sequencer from Life Technologies. Antibodies for ChIP-seq: Anti-Hdac3 (Abcam ab7030), p300 (Santa Cruz sc-585), Olig2 (Millipore AB9610), Histone 3 Ac-K27 (Active Motif 39133).

Procedure for lysolecithin-induced demyelinating injury: Lysolecithin-induced demyelination was carried out in the ventrolateral spinal white matter of 8-week-old wildtype mice as previously described (Keough et al., 2015). Anesthesia was induced and maintained by peritoneal injection of a mixture of ketamine (90 mg/kg) and xylazine (10 mg/kg). After exposing the spinal vertebrae at the level of T9-T12, meningeal tissue in the intervertebral space was cleared, and the dura was pierced with a dental needle. was advanced through the pierced dura and 0.5 μL of 1% lysolecithin (L-a-lysophosphatidylcholine, sigma) via a Hamilton syringe attached a glass micropipette was injected into the ventrolateral white matter via a stereotactic apparatus.

SUPPLEMENTARY REFERENCES

Chan, J.R., Watkins, T.A., Cosgaya, J.M., Zhang, C., Chen, L., Reichardt, L.F., Shooter, E.M., and Barres, B.A. (2004). NGF controls axonal receptivity to myelination by Schwann cells or oligodendrocytes. Neuron *43*, 183-191.

Chen, Y., Balasubramaniyan, V., Peng, J., Hurlock, E.C., Tallquist, M., Li, J., and Lu, Q.R. (2007). Isolation and culture of rat and mouse oligodendrocyte precursor cells. Nature protocols *2*, 1044-1051.

Keough, M.B., Jensen, S.K., and Yong, V.W. (2015). Experimental demyelination and remyelination of murine spinal cord by focal injection of lysolecithin. J Vis Exp.

Lu, Q.R., Sun, T., Zhu, Z., Ma, N., Garcia, M., Stiles, C.D., and Rowitch, D.H. (2002). Common developmental requirement for Olig function indicates a motor neuron/oligodendrocyte connection. Cell *109*, 75-86.

Lu, Q.R., Yuk, D., Alberta, J.A., Zhu, Z., Pawlitzky, I., Chan, J., McMahon, A.P., Stiles, C.D., and Rowitch, D.H. (2000). Sonic hedgehog--regulated oligodendrocyte lineage genes encoding bHLH proteins in the mammalian central nervous system. Neuron *25*, 317-329.

McCarthy, K.D., and de Vellis, J. (1980). Preparation of separate astroglial and oligodendroglial cell cultures from rat cerebral tissue. J Cell Biol *85*, 890-902.

Weng, Q., Chen, Y., Wang, H., Xu, X., Yang, B., He, Q., Shou, W., Higashi, Y., van den Berghe,

V., Seuntjens, E.*, et al.* (2012). Dual-mode modulation of Smad signaling by Smad-interacting protein Sip1 is required for myelination in the central nervous system. Neuron *73*, 713-728.

Ye, F., Chen, Y., Hoang, T., Montgomery, R.L., Zhao, X.H., Bu, H., Hu, T., Taketo, M.M., van Es, J.H., Clevers, H.*, et al.* (2009). HDAC1 and HDAC2 regulate oligodendrocyte differentiation by disrupting the beta-catenin-TCF interaction. Nat Neurosci *12*, 829-838.

Yu, Y., Chen, Y., Kim, B., Wang, H., Zhao, C., He, X., Liu, L., Liu, W., Wu, L.M., Mao, M.*, et al.* (2013). Olig2 targets chromatin remodelers to enhancers to initiate oligodendrocyte differentiation. Cell *152*, 248-261.